

72320 Roversystemtechnik
Summer Semester 2021

INSPIRE

IN-situ Sampling and Primal Investigation Rover on Europa

Phase 0/A-Study of a Rover Mission on the Surface of the Jupiter moon Europa

Denis Acker
Daniel Bölke
Korbinian Kasper
Christian Korn
Nicolas Probst
Saskia Sütterlin

Supervisors:
Moritz Nitz M.Sc.
Patrick Winterhalder M.Sc.

University of Stuttgart
Institute of Space Systems
Prof. Dr. Sabine Klinkner
18.07.2021

Symbols

Symbol	Definition	Unit
a	Constant for the Geometry of a Porous Media	nm
A	Wheel Ground Contact Area	m
b	Wheel Width	m
c	Coefficient of Soil Cohesion	Pa
$C_{\text{Batt,req}}$	Total Required Battery Capacity	Wh
$C_{\text{Batt,req}}$	Battery Nominal Capacity	Wh
C_{cell}	Cell Voltage	V
C_{rr}	Rolling Resistance Coefficient	-
d	Wheel Diameter	m
DoD	Depth of Discharge	%
DP	Drawbar Pull	N
H	Soil Thrust	N
h_{Ice}	Ice Crust Surface Thickness on Europa	m
k_c	Sinkage Modulus	$\frac{\text{kN}}{\text{m}^{n+2}}$
k_ϕ	Soil Friction Angle Sinkage Modulus	$\frac{\text{kN}}{\text{m}^{n+3}}$
l	Ground Contact Length	m
T_{Surface}	Surface Temperature on Europa	K
M	Number of Cells in Parallel	-
m_{RTG}	RTG Mass	kg
n	Soil Deformation Exponent	-
N	Number of Cells in Series	-
P_{el}	RTG Electrical Power	W_{el}
$P_{\text{el,req}}$	Required Electrical Power	W_{el}
P_{mode}	Demanded Electrical Power per Mode	W_{el}
R_b	Bulldozing Resistance	N
R_c	Compaction Resistance	N
R_g	Gravitational Resistance	N
R_r	Rolling Resistance	N
t_e	Mode Duration	s
W_{wheel}	Normal Force per Wheel	N
z	Sinkage	m
α_{BOL}	BOL Specific Power	$\frac{W_{\text{el}}}{\text{kg}}$
ϵ	Emissivity	-
η_{LiIon}	Efficiency of LiIon Cells	-
ϕ	Friciton Angle	°
ρ_{Ice}	Inner Encoder Ring Diameter	$\frac{\text{kg}}{\text{m}^3}$
θ	Slope Angle	°

Abbreviations

BOL	Begin of Life
BOM	Begin of Mission
COMM	Communications
DoD	Depth of Discharge
EOM	End of Mission
EPS	Electrical Power System
2D	Two Dimensional
3D	Three Dimensional
PCDU	Power Control and Distribution Unit
PCU	Power Control Unit
PDU	Power Distribution and Control Unit
IMU	Inertial Measurement Unit
IRS	Institute of space Systems at the University of Stuttgart
INSPIRE	IN-situ Sampling and Primal Investigation Rover on Europa
ESA	European Space Agency
MMP	Mean Maximum Pressure
NASA	National Aeronautics and Space Administration
SPENVIS	SPace ENVironment Information System
HPC	High Priority Commands
RTG	Radioisotope Thermoelectric Generator
eMMRTG	Enhanced Multi Mission Radioisotope Thermoelectric Generator
eSMMRTG	Enhanced and Scaled Multi Mission Radioisotope Thermoelectric Generator (3kg)
TID	Total Ionizing Dose
OBC	On-Board Computer
S/C	

Contents

Symbols	I
Abbreviations	II
List of Figures	V
List of Tables	VI
1 The Mission	1
2 Payload	2
2.1 Sterovision Camera / Observation / Perception	2
2.2 Ground RADAR	2
2.3 Ice Core Drill	2
2.4 RadHard Solar Arrays	2
3 Operation	3
3.1 Mission Phases	3
3.1.1 Rover System Modes	3
4 Subsystems	6
4.1 Rover	6
4.2 Structure and Mechanics	6
4.3 Communications and Command and Data-Handling	6
4.4 Payload	6
4.5 Thermal Control System	7
4.5.1 Thermal concepts	7
4.5.2 Thermal Network	8
4.5.3 Thermal analysis	9
4.5.4 Results	9
4.6 Electrical Power System	11
4.6.1 EPS Budget and Overview	11
4.6.2 Energy Source	12
4.6.3 Energy Storage	12
4.6.4 EPS Power Control and Distribution	13
4.7 Radiation	14
4.7.1 Radiation Protection	14
4.7.2 Components	14
4.7.3 Improvements	15
4.7.4 Conclusion	15
4.8 Locomotion	16
5 Outlook	17
Appendix	19
A Electrical Power System	19
B Thermal Controls System	21
B.1 Heat energy equilibrium	21

	B.2	Heat conductance	22
	B.3	Heat switch	22
	B.4	Rover absorptivity	23
	B.5	Values	24
C		Radiation	26
	C.1	Jupiters Radiation Environment	26
	C.2	Radiation Exposures	27
	C.3	Improvements	28

List of Figures

3.1	Preliminary Mission Timeline for INSPIRE.	3
4.1	Carbon-based thermal strap <i>LyNX</i> [®]	7
4.2	Heat switch.	8
4.3	Change of the heat switch conductivity R_t over the mean temperature T_M	8
4.4	Thermal network of the rover.	9
4.5	Functional Flow Chart Diagram for the EPS Subsystem.	11
4.6	Overview of TIDs within different compartments within the rover.	15
A.1	POWER BUDGET DUMMY!	20
B.2	Switch characteristic divided in sections.	23
C.3	Average trapped proton and electron fluxes on an orbit around earth at 25,000 km, through the outer Van Allen radiation belt, and on Europa's orbit around Jupiter.	26
C.4	TID of aluminium, titanium, and the optimised radiation structure shown in Table 4.5 with a weight target of all three structures of 0.5 g/cm ² over 30 days of exposure on Europa.	27
C.5	TID for different compartments as seen in Figure 4.6. The E-Bay is shielded by 4 mm aluminium, 0.415 mm lead, and 0.033 mm iron; the camera compartment by 2 mm aluminium, 0.415 mm lead, and 0.033 mm iron; the chassis by 2 mm aluminium; the electric motors by 1 mm aluminium.	28
C.6	TID with 4 mm Al shielding over a mission duration of 30 days	28
C.7	TID with 4 mm Al shielding and 1 cm of Water over a mission duration of 30 days	29

List of Tables

3.1	Collection of Rover System Modes. [Kommt noch in Anhang]	5
4.1	Temperature results in K of thermal analysis, including a margin of $\pm 15K$.	10
4.2	Overview of the Power Budget of INSPIRE.	11
4.3	Parameters for the scaled eSMMRTG based on the eMMRTG.	12
4.4	Power consumption mode used as design case for the battery sizing.	13
4.5	Optimal shield structure for an Jupiter mission. [Platzhalter]	14
A.1	INSPIRE battery parameters.	19
B.2	Sections and range of the switch characteristic.	23
B.3	Temperatur limits of the rover components.	24
B.4	Minimum and maximum of surface emisivity and absorptivity values.	24
B.5	Heat conductivity in $\frac{W}{mK}$	25
B.6	Radiation surface of components.	25
C.7	Used components and the respective radiation tolerance and location	27

Chapter 1

The Mission

During the observation of Jupiter, the Glileo spacecraft did also some flybys of the Jupiter moons. The scientist gahtered data from Europa, which suported the evidence of a thick icy surface. The possibility of liquid water underneath lead astrobiologists to the assumption that extraterrestrial life could exist on Europa. That is why Europo is - beside Mars - an interesting object of research.

Therefore, the ESA will launch the *JUICE* oriber in 2022 to investigate Europa in more detail. But also the NASA is developing *Europa Clipper* to get detailed information. Additionally, they plan a lander for Europer to bring scientific instruments onto the surface. The DLR will perform the side mission TRIPLE, with project coordinator Dr. Waldmann, which take samples of the water by melting through the ice with an special testing probe.

Under the leadership of Prof. Dr.-Ing. Klinkner, the Institute of Aero Space Systems started within a seminar a feasibility study about a rover system to explore Europa surface, which shall be part of the *TRIPLE* mission. This challenge was given to five student teams in order to develop concepts, construct preliminary designs, perform analysis and make evaluations to meet the mission objectives and fit the mandatory requirements cite.

This report contain the results of the Phase A study of the rover system IN-SITU SAMPLING AND PRIMAL INVESTIGATION ROVER ON EUROPA (INSPIRE).

Chapter 2

Payload

2.1 Sterovision Camera / Observation / Perception

The INSPIRE rover is equipped with five individual cameras. Two are used as stereo vision cameras on an hight adjustable and rotatable telescope arm on the front side of the rover. This ist used to capture a detailed 3D model of the environment with which sizes and distances can be estimated. The remaining three cameras are used as has-cameras which are necessary to obtain data regarding the nearby environment. All cameras are equipped with radiation hardened lenses to prevent browning of the lenses. The main tasks of the camera system is the provision of scientific data and navigation related data. More details regarding the navigation and autonomy are provided in ??.

2.2 Ground RADAR

2.3 Ice Core Drill

2.4 RadHard Solar Arrays

As a secondary mission goal for INSPIRE a cooperation with the european project RadHard which is led by the german solar array manufacturer Azure Space is intended. They are currently developing a new generation of 4 Junction solar cells with an efficiency of up to 35%. But the main feature of the new solar arrays is their radiation hardness which will be the highest radiation hardness ever designed with an efficiency of $> 3\%$ after $1E15\text{ cm}^{-2}$ 1MeV electron irradiation. So the Jupiter environment with its extreme radiation would be the best suitable destination for a test and evaulation mission of this new technology. Therefore INSPIRE will be equipped with 8 RadHard solar cells with a total surface area of 0.0248m^2 for a technology demonstration[1].

Chapter 3

Operation

.....

3.1 Mission Phases

For the INSPIRE Mission Phase 0 study five basic mission phases have been defined. Furthermore a sixth optional mission phase after the nominal mission lifetime has been established which will be conducted if the rover is still operational after its nominal lifetime.

- **Phase 0:** Launch and Flight Phase
- **Phase 1:** Entry, Descent and Landing Phase
- **Phase 2:** Depolymment Phase
- **Phase 3:** Egress, Comissioning and Early Operation Phase
- **Phase 4:** Mission Operation Phase
- **(Phase 5:** Exceeding Mission Operation Phase)

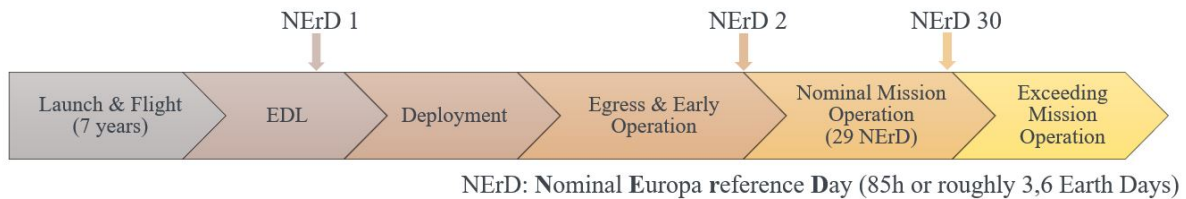


Figure 3.1: Preliminary Mission Timeline for INSPIRE.

Based on these missions phases some preliminary rover system modes as well as a basic mission timeline were concluded.

3.1.1 Rover System Modes

For this case study several rover system modes were defined. All ten modes are listed in Table 3.1. They are separated into two groups. The design critical modes are displayed in white and are defined as system modes, which significantly influence the preliminary design of the rover subsystem like the thermal or power subsystem. None design critical modes (grey) also have a major influence on multiple subsystems of the rover but play a secondary role in the thermal and power budget of the rover for this Phase 0 study. These non design critical modes extend from the rover storage and launch until the finale deployment of the rover is completed. These modes and their design options depend heavily on the final design of the lander with which INSPIRE flies to Europe. Therefore, a clear definition of such modes is not possible at this time in the course of this phase 0 study. However, the respective considerations, preferences and options have been briefly described in the mode descriptions. It is important to note that INSPIRE's

goal is to provide a flexible rover design with as few hard requirements as possible for the parent lander. Therefore, many aspects of the rover, as well as the none design critical modes, will need to be further defined and elaborated in later phases of the project in close consultation with the customer.

For example, the exact interfaces between rover and lander should be defined in more detail. Depending on the subsequently chosen interfaces, many possibilities may arise in the corresponding rover system modes. With an appropriate interface, for example, the excess electrical and thermal energy of the RTG, which is already active during the flight, could be used to supply the lander system with heat and power. A corresponding interface could also enable the transmission of health checks from INSPIRE.

The deployment phase will strongly depend on the final design of the lander, INSPIRE's position within the lander and also the possibilities that the lander provides to INSPIRE. Possible deployment strategies would be as follows:

- **Option 1:** If INSPIRE on ground level: Release from storage box through spring mechanism or actuators. Rover storage configuration allows rolling and possible motorized actuation

- **Option 2:** If INSPIRE is above ground level: Similar as Option 1 but an additional ramp and ramp deployment would be required.

- **Option 3:** INSPIRE will be deployed through the lander's robotic arm if it is capable of lifting its mass.

Number	Rover System Modes	Abbreviation	Definition
0	Launch/Off Mode	OFF	From Launch until EDL Phase Rover System is OFF Exact mode description t.b.d. and can be adapted to meet the lander demands Health tests on Occasion during flight time are foreseen (PCDU could be active) Batteries on Storage Capacity at launch and may be recharged on occasion (like Rosetta Mission) Telemetry data shall be sent by the Lander (optional if possible) RTG on =>Electrical and Thermal Power may be used (for Lander Power and Thermal Systems) or is disposed of by shunts From Entry until next morning after secure landing of Lander on Europa See Mode OFF
1	Entry, Descent and Landing	EDL	PCDU ON after secure landing (Powered by RTG) Heaters ON (powered by remaining RTG Power) Battery charging if no Kill Switch is used
2	Deployment and Early Operation Mode	EOP	First Morning after EDL Exact mode description t.b.d. and can be customized to lander =>Dependant on final Lander Design Critical Deployments (Egress System) and leaving the lander Optional whether Kill Switch ejected =>Battery charging can start Rover System Activation possibilities: Kill Switch, Lander Interface, HPC from Earth PCDU ON OBC ON Heaters ON After sufficient Battery Capacity is reached (50%): Deployment of Rover Boogie and checkout/health check of all Rover Systems Afterward switching to Charging Mode
3	Idle/ Perception	ID	During Idle Operation Time Rover powered by RTG or Batteries (Excess Power charges Batteries) PCDU ON All Components in Standby or Power Saving Mode if possible Stereovision Camera ON for Orientation and Observation (Science Data) Hazcams and OBC ON for Orientation and Path Analysation COMM ON for larger time intervals (Listening Mode)
4	Safe Mode/ Hibernation (SAFE)	SAFE	Entered in case of emergency or contingency Rover Survival Mode =>Minimum Power PCDU ON COMM sends Emergency Signal then switches to COMM ON for small time intervals (Listening Mode) OBC OFF until Command received =>High Power Commands (HPC) Heaters ON Science data shall be stored without data loss Applicable during Day and Nighttime Exit after receiving the corresponding command (Optional: Timer ON and Restart of Rover System after time period has passed)
6	Communication	COMM	During Transmission of major Telemetry or Science Data Rover powered by RTG or Batteries (Excess Power charges Batteries) PCDU ON All Components in Standby or Power Saving Mode if possible OBC SB COMM ON (Transmission Mode)
7	Charging	BAT	For Battery charging Rover batteries charged by RTG PCDU ON All Components in Standby or Power Saving Mode if possible OBC SB Quit after sufficient charge is reached
8	Locomotion	LOC	For Rover Movement and Observation Locomotion and Navigation ON Hazcams and Traversing Path Analysis ON OBC ON PCDU ON COMM OFF Stereovision Camera ON for Orientation and Observation (Science Data) Only during Daytime
9	Payload Observation Mode	OBS	Payload Mode for Science Data Collection during Daytime OBC ON PCDU ON COMM OFF Stereovision Camera ON for Orientation and Observation (Science Data) RADAR ON for Ground Investigation =>Drill Location Only during Daytime
10	Payload: Ice Core Mode	ICE	Payload Mode for Science Data Collection during Daytime or Nighttime OBC ON PCDU ON COMM OFF Ice Core Drill ON during Ice Core Sample Collection Afterwards Sample will be analysed =>APXS ON

Table 3.1: Collection of Rover System Modes. [Kommt noch in Anhang]

Chapter 4

Subsystems

.....

4.1 Rover

...

4.2 Structure and Mechanics

...

4.3 Communications and Command and Data-Handling

...

4.4 Payload

...

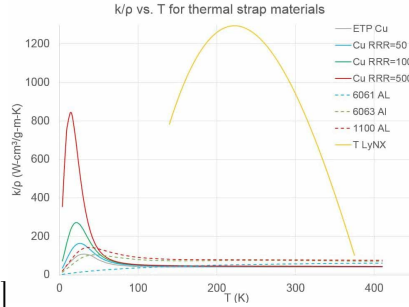
4.5 Thermal Control System

The main object of the Thermal Control System (TSC) is to keep the electric components within their temperature limits, listed in Table B.3. As a result of Europas low ground temperature, a small solar constant and the thin atmosphere the heat loss of the rover has to be minimised. This shall be reached by a smart heat distribution as well as by an adequate insulation and surface finishing.

4.5.1 Thermal concepts

The main heat source of the rover is the waste heat of the RTG (see Section 4.6), which will be lead by thermal straps to the thermal critical components. The first attempt to use straps made out of copper was rejected due to the high resulting mass. Therefore, carbon-based straps (Thermal LyNX) with a high thermal conductivity to density ratio will be used, cite. However, the thermal conductivity is highly depend on the materials temperature, see ???. The curve was approximated by an cubic interpolation, autoref appendix. To consider heat loss as a result of contact and radiation, the thermal conductivity was reduced about 20%.

[Temperature dependent thermal conductivity/density of *LyNX*[®] (yellow curve), copper, and



aluminum, cite.]

[Example of a thermal



strap.]

Figure 4.1: Carbon-based thermal strap *LyNX*[®].

The camera, exposed on a mast, will be heated by a separate, light weight Radioisotope Heater Unit (RHU), citeRHU, which has been used during several NASA missions. For the insulation, the material *aerogel* will be applied, which has a very low heat conductivity (cite aerogel) as well as a low density and has also been used in space applications (citeaerogel).

A surface finishing with a low emissivity is necessary. For the most componets, a cost-efficient surface polishing is applicable. The camera will get a special white paint with a high absorptivity to gather the sun light.

But ther is also a risk of overheating, because of the lack of heat convection. This circumstance concern the engines and also the camera. To get rid of the extensive heat and prevent the damage of the components special heat switches will be placed (see Figure 4.2). These switches change their heat conductivity beyond a certain temperatur due to the expansion of the disk (see Figure 4.3). It was assumed, that the toggle temperatur can be adapted by increasing the disk height. The influence of the changed disk stiffens on the contact pressure and the heat conductivity was neglected for this study. The measured heat conductivity characterisitc was

divided in three linear sections (Figure ??), to enable a simple modelling in the upcoming thermal calculation.

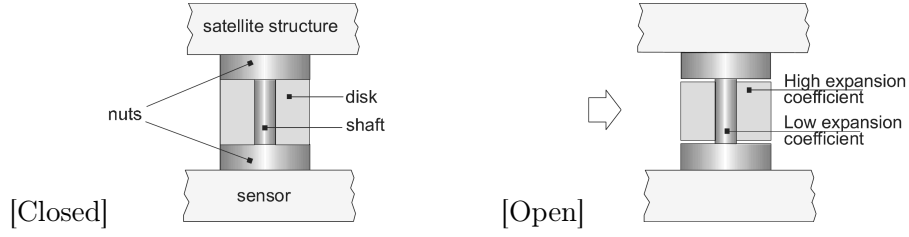


Figure 4.2: Heat switch.

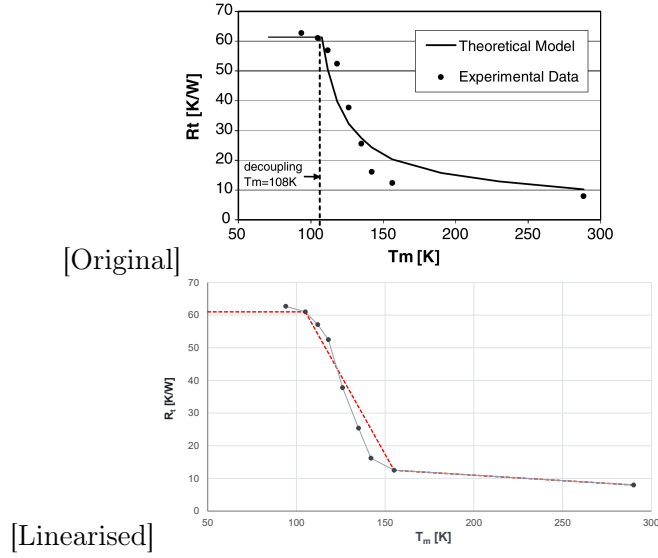


Figure 4.3: Change of the heat switch conductivity R_t over the mean temperature T_M .

4.5.2 Thermal Network

A thermal analysis was performed in order to get

- the dimension of the insulation and heat straps,
- the necessary amount of RHUs and heat switches,
- the required surface finishing.

For that, a thermal network with ten nodes was derived from the rover, shown in Figure 4.4. At the intersection of the steering and drive engine, two additional nodes were defined to calculate the heat flow.

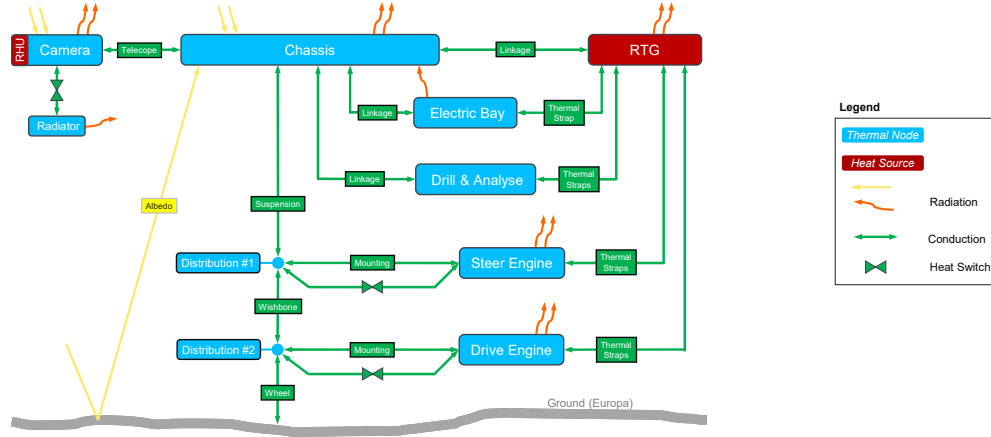


Figure 4.4: Thermal network of the rover.

On the basis of the thermal network, the heat energy equilibrium for each node was defined (see Section B). The calculation were considered as a quasi-static analysis, where the component temperatures stay constant, $\frac{dT}{dt} = 0$. Due to the early state of the rover, simplifications and assumptions were made.

- The convection was neglected due to the thin atmosphere.
- The whole electrical power of the components will be dissipated into heat.
- A variation of $\pm 20\%$ for the emissivity and absorptivity values was considered, if applicable (see Table B.4).
- The heat as a result of retardation radiation inside the shielding was neglected.
- The E-Bay emits heat energy only in one direction to the chassis.
- Only the chassis and the camera absorb sun radiation, detailed description see Subsection B.4.
- The ice core drill and the APXS analyser were summarised as one single node.
- No discrete nodes for the radar, hazcams and deployment engines were considered. Their heat will be lead into the chassis.
- The thermal resistance between two surfaces and their radiation of the thermal strap was neglected. To compensate this assumption, the heat conductivity was reduced about 20%.

4.5.3 Thermal analysis

The thermal analysis was performed as a Excel calculation, which can be found in the corresponding folder of Team 3. The calculation sheet offers the possibility to adapt and customise input values and dimension.

4.5.4 Results

The results of the temperatures for each node at each for the hot and cold cases are listed in autoreftab:. The temperature margins for uncertainties, acceptance tests and qualification tests were considered with $5K$ each, $\pm 15K$ in total. The corresponding temperatures are listed in autoreftab:. All temperature lay between their limits without using a heater. Nevertheless, heaters were considered for the power calculation, see Section 4.6.

Components	Load Case			
	Hot case		Cold case	
	0K	+15K	0K	-15K
RTG	380	395	350	335
Electric Bay	310	325	261	246
Drill & Analyser				
Camera				
Steering Engine				
Drive Engine				

Table 4.1: Temperature results in K of thermal analysis, including a margin of $\pm 15K$.

In a further step, a more detailed analysis has to be carried out with the Finite-Element-Method to identify the correct heat and temperature distribution. The FE results could be used to verify and adjust the analytical analysis to get a helpful tool for fast thermal calculation to evaluate different materials or designs in the further development phases.

4.6 Electrical Power System

The EPS (Electrical Power System) is the subsystem responsible for the electrical power supply of INSPIRE. It consists of four fundamental parts, which are the energy source, the PCDU unit (Power Control and Distribution) and the Energy Storage as well as the rover subsystems as the consumers. The EPS is visualized in Figure 4.5.

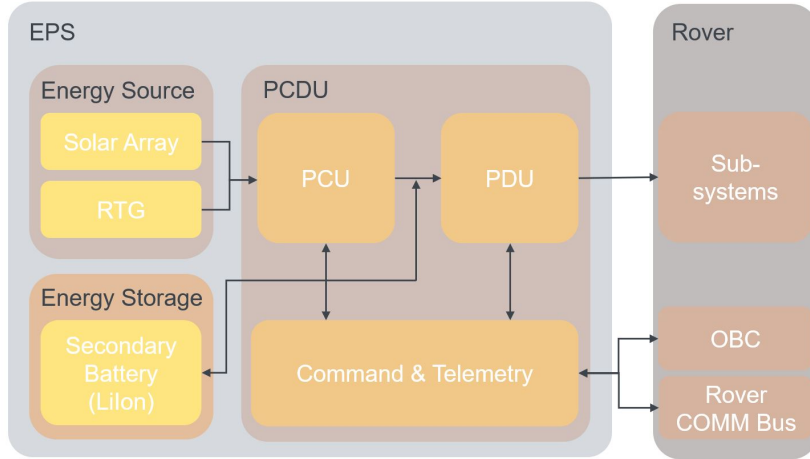


Figure 4.5: Functional Flow Chart Diagram for the EPS Subsystem.

4.6.1 EPS Budget and Overview

Table 4.2 summarizes the power budget of INSPIRE based on the rover system modes defined in Subsection 3.1.1. The complete power budget can be found in Figure A.1. As can be seen, the Locomotion mode has the highest demands on the EPS. Communication mode also has a high consumption. However, since this is primarily used at night and the rover can be charged again afterwards without any problems, it does not place any major restrictions on the power budget. Idle/Perception mode has a low consumption, but is usually used for a long time at a stretch and therefore also places high demands on the EPS. In Charging mode, the EPS is able to charge $7.04 W_{el}$.

Rover System Mode	Total Rover Power Demand including battery charge $P_{mode} [W_{el}]$
Idle/Perception	15.25
Safe/Hibernation	-5.84
Communication	36.92
Charging	-7.04
Locomotion	232.36
Payload: Observation	15.41
Payload: Ice Core Mode	9.77

Table 4.2: Overview of the Power Budget of INSPIRE.

4.6.2 Energy Source

For the energy generation of INSPIRE many possible sources were taken into consideration for a trade-off. As a conclusion of this trade-off the decision was made to utilize a Radioisotope Thermoelectric Generator (RTG) as the main energy source for INSPIRE.

As the research couldn't find an RTG with a mass suitable for INSPIRE, the solution was to scale down a bigger RTG as an approximation. As a baseline of the scaling the eMMRTG (Enhanced Multi Mission Radioisotope Thermoelectric Generator) was utilized, which is currently under development at NASA and is especially designed for deep space missions like Europa. For the scaling a goal RTG mass of $m_{\text{RTG}} = 3 \text{ kg}$ was defined and the eMMRTG was scaled down using the given data.

In Table 4.3 the scaling results for the eSMMRTG (Enhanced and Scaled Multi Mission Radioisotope Thermoelectric Generator) are listed. The eSMMRTG has a BOL specific power of $\alpha_{\text{BOL}} = 4.0 \frac{W_{el}}{kg}$ and provides an electrical power of $P_{el} = 12.08 W_{el}$ during the mission duration[2][3][4][5][6].

Scaled eSMMRTG Parameter	
System Mass m_{RTG} [kg]	3.5
BOL Specific Power $\alpha_{\text{BOL}} \frac{W_{el}}{kg}$	4.0
BOL Power $P_{el,\text{BOL}} W_{el}$	14
Isotop	Pu-238
Isotop Half-Life [a]	87.7
Flight time and Storage (incl. Margins) [a]	7
Power Loss Degradation until BOM W_{el}	0.56
BOM Power $P_{el,\text{BOM}} W_{el}$	13.44
Europa Day Duration [h]	85
Mission Duration [d]	106.25
End of Mission Power $P_{el,\text{EOM}} [W_{el}]$	13.42
Final Power for Study $P_{el} [W_{el}]$ (incl. 10% scaling Margin)	12.08

Table 4.3: Parameters for the scaled eSMMRTG based on the eMMRTG.

Furthermore INSPIRE will also be equipped with some radiation hardend solar arrays as already explained in Section 2.4[1]. Since these solar cells are primarily used for technology testing, the mission must also be able to operate completely without this generated energy. For this reason, and because the expected energy generated by the solar cells is minimal, only the energy generated by the RTG is considered for the Phase 0 Study. However, it should be noted that these solar cells will also generate a certain amount of energy, which will be beneficial for the EPS.

4.6.3 Energy Storage

For the energy storage of INSPIRE many possible battery types were taken into consideration for a trade-off. As a conclusion of this trade-off the decision was made to utilize LiIon batteries as the secondary batteries of INSPIRE. This decision is primarily based on LiIon batteries high energy density, temperature range, robust performance and long operating and cycle life in extreme environments[7].

As the RTG only generates a small constant power the main energy source during the mission will be the accumulated energy of the batteries. The rover will charge the batteries at night,

so the next exploration day can start with full capacity. Furthermore the batteries have to be charged during day time to maintain operations.

For the sizing of the batteries, the rover motion was chosen as the design driver, since this is the highest energy consuming state of the rover and additionally mission critical for INSPIRE. The rover motion consists of an interaction of the Locomotion and Perception mode as already mentioned in Chapter 3. Therefore it was defined that INSPIRE shall be able to drive 50 *m* (including alternating Locomotion and Perception Mode) with a fully charged Battery. The required battery capacity $C_{\text{Batt,req}}$ can be calculated using Equation 4.1. The results are listed in Table 4.4 [8].

$$C_{\text{Batt,req}} = \frac{P_{\text{el,req}} \cdot t_e}{DoD \cdot \eta_{\text{LiIon}}} \quad (4.1)$$

Power Consumption Mode:	Locomotion	Perception
Required Electrical Power $P_{\text{el,req}}$ [<i>W_{el}</i>]	283.43	14.01
Duration of the mode t_e [<i>s</i>]	500	15000
<i>DOD</i> for Dimensioning [-]	0.90	0.90
Efficiency of LiIon Cells η_{LiIon} [-]	0.95	0.95
Required Battery Capacity per mode C_{mode} [<i>Wh</i>]	46.04	68.27
Total Required Battery Capacity $C_{\text{Batt,req}}$ [<i>Wh</i>]	114.32	

Table 4.4: Power consumption mode used as design case for the battery sizing.

Using these values a suitable battery cell and battery design configuration were conducted. Under consideration of these parameters the battery capacity C_{Batt} can be calculated:

$$C_{\text{Batt}} = C_{\text{cell}} \cdot V_{\text{cell}} \cdot N \cdot M. \quad (4.2)$$

According to the ECSS reliability restrictions 1 battery string must be subtracted for dimensioning. Furthermore a 30% margin on the energy content was applied. This leads to a final battery configuration with a capacity of $C_{\text{Batt}} = 138,88 \text{ Wh}$ and a mass of $m_{\text{Batt}} = 1980 \text{ g}$. The final battery values are listed in Table A.1 [9].

4.6.4 EPS Power Control and Distribution

In order to ensure the full functionality of the EPS, the last main component to be selected is a suitable PCDU. As described in Figure 4.5, the PCDU forms the heart of the EPS and is an important interface to the OBC and COMM. Furthermore the PCDU shall be able to monitor and control the rover system if necessary through watchdogs, HPC (High Priority Commands) and direct connections to the OBC and COMM.

The PCDU has the challenging task not only to process the RTG as the main energy source, but also to process solar cells as secondary energy sources. Therefore, a PCDU was sought which has the required size, dimensions and range of functions. The research resulted in the Nova PCDU from Bradford DSI. In addition, margins were added to the PCDU to ensure feasibility[10].

4.7 Radiation

Compared to the radiation environment near Earth the radiation environment near Jupiter is multiple times stronger. It has the highest radiation levels of any planet in our solar systems [Platzhalter]. In order to survive these harsh environmental conditions, special emphasis must be placed on the radiation protection. In Figure C.3, the average trapped proton and electron fluxes on Europa's orbit around Jupiter are shown in comparison to the outer Van Allen radiation belt around Earth. However, in contrast to the Van Allen radiation belt, the duration within the radiation environment on Europa cannot be minimised and the rover has to be designed to withstand the entire mission duration of 30 days.

In order to design and evaluate different radiation protection approaches, different calculations have to be performed. For this purpose the ESA SPace ENVironment Information System (SPENVIS) is used [Platzhalter]. All calculations and figures in Section 4.7 are performed with SPENVIS unless otherwise stated.

4.7.1 Radiation Protection

Various options are available to protect the rover against the radiation. A common approach is the use of aluminium or titanium as these materials can also act as structural elements. However, due to the mass constraints of 30 kg other materials or material compositions are taken in consideration which are more mass effective. In Table 4.5, an optimised shield structure is presented for different weight thresholds designed for the radiation environment around Jupiter. The difference between an aluminium or titanium shielding and an optimised structure listed in Table 4.5 for the total ionizing dose (TID) is shown in Figure C.4.

Due to the mass savings of the optimised structure it will be used where the radiation protection of the aluminium structure is not sufficient. In order to reduce the mass further, a radiation vault is utilised that highly sensitive components do not have to be shielded separately.

Table 4.5: Optimal shield structure for an Jupiter mission. [Platzhalter]

Areal Density / g/cm ²	0.5	1	2	3
Layer No. 1	Pb	Pb	W	Ta
/ mm	0.415	0.829	0.984	1.563
Layer No. 2	Fe	Mg	Mg	Al
/ mm	0.033	0.158	0.540	0.399
Layer No. 3	-	-	-	Mg
/ mm	-	-	-	0.150

4.7.2 Components

Every component on the rover has a different radiation tolerance and therefore have to be placed at different compartments within the rover. The radiation tolerances are listed in Table C.7. None sensitive components like the electric motors and harness are only shielded by an aluminium structure where components like the metal within the wire are resistant against the radiation. However, isolators around the cables have to be selected to be resistant in order to prevent short circuits. Highly sensitive components like cameras have an additional protective layer in order to reduce the TID to under 30 krad. Components which are within the rover like the on-board computer (OBC) are placed within the radiation vault which reduces the TID to under 20 krad. For this purpose the optimised shield structure with a weight target of 0.5 g/cm² is used. Detailed TIDs for all components are shown in Figure C.5.

4.7.3 Improvements

Even though the radiation protection is sufficient for the rover to survive at least the nominal mission of 30 days, further improvements can be performed in order to extend the secondary mission.

Local shielding can be applied on less resistant components in order to reduce the wall thickness of the whole radiation wall. If components with a radiation tolerance under 43.27 krad are individually shielded a mass saving of 736.2 g can be achieved. Additionally, water ice extracted from the surface of Europa can be used to improve the radiation protection. With a layer of one centimetre of water, the TID within the radiation vault can be reduced to 16.03 krad without the additional radiation protection beside the 4 mm of aluminium structure. The start mass of the rover can therefore be reduced by 897.2 g by removing the additional shielding.

Detailed calculations for local shielding and water improvements can be found in Subsection C.3 and may be analysed further in Phase B.

4.7.4 Conclusion

In order to protect the rover against the high radiation levels at the surface of Europa, the rover has different compartments. High sensible components are placed within a radiation vault which has a mass optimised structure. Components which has to be outside the radiation vault but are highly sensible are shielded individually. Low sensible Components are protected by the Aluminium structure. Figure 4.6 illustrates the different compartments within the rover and the accorded TIDs.

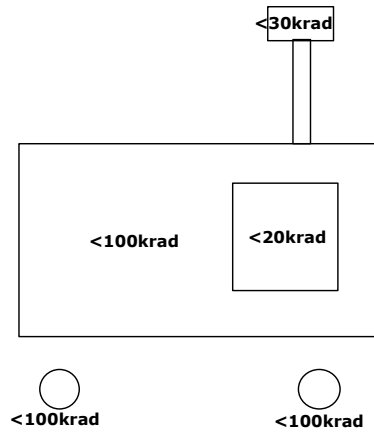


Figure 4.6: Overview of TIDs within different compartments within the rover.

4.8 Locomotion

The locomotion subsystem deals with the aspect of how the rover moves and the technical design, including the selection of components such as motors or gearboxes. Before the components can be determined, however, it is necessary to consider certain parameters. These parameters will be introduced in the following, and the decisions or estimations concerning the rover will be presented.

Design drivers

Regarding techniques of rover movement, it is crucial to consider the local conditions in which the rover will be operating. The surface of Europa can be assumed to be mainly covered by ice. However, since there are also geysers that transport water to the surface, surface areas may be covered by snow. Though Europa's surface temperature does not exceed 130 K, rather icy, hard-packed snow can be assumed. For this study, a conservative design of the rover is considered, whereby material parameters of snow in Sweden were selected, see ?? Furthermore, a 4-wheeled rover is chosen, as evidenced by a trade-off in

Chapter 5

Outlook

Bibliography

- [1] Fraunhofer Institute for Solar Energy Systems ISE. *RadHard Project Website*. 2021. [online] [\url{https://radhard.org/}](https://radhard.org/).
- [2] R. Abelson et al. *Enabling Exploration with Small Radioisotope Power Systems*. Ed. by NASA JPL. 2004.
- [3] S. Magdum. *Model Based Development of The Enhanced Multi-Mission Radioisotope Thermoelectric Generator and Effect of Thermoelectric Element Length on eMMRTG*. Ed. by Western Michigan University. 2019. [online] [\url{http://homepages.wmich.edu/~leehs/ME539/Final%20Presentation%20on%20eMMRTG.pdf}](http://homepages.wmich.edu/~leehs/ME539/Final%20Presentation%20on%20eMMRTG.pdf).
- [4] Holgate, T. C.; Bennett, R.; Hammel, T.; Caillat, T.; Keyser, S., and Sievers, B. “Increasing the Efficiency of the Multi-mission Radioisotope Thermoelectric Generator”. In: *Journal of Electronic Materials* 44.6 (2015), pp. 1814–1821. ISSN: 0361-5235. DOI: [\url{10.1007/s11664-014-3564-9}](https://doi.org/10.1007/s11664-014-3564-9).
- [5] JPL NASA. *Enhanced Multi-Mission Radioisotope Thermoelectric Generator (eMMRTG) Concept*. Ed. by NASA JPL. 2014. [online] [\url{https://rps.nasa.gov/resources/56/enhanced-multi-mission-radioisotope-thermoelectric-generator-emmrtg-concept/}](https://rps.nasa.gov/resources/56/enhanced-multi-mission-radioisotope-thermoelectric-generator-emmrtg-concept/).
- [6] Lakdawalla, E. *The Design and Engineering of Curiosity*. Cham: Springer International Publishing, 2018. ISBN: 978-3-319-68144-3. DOI: [\url{10.1007/978-3-319-68146-7}](https://doi.org/10.1007/978-3-319-68146-7).
- [7] S. Fasoulas et al. *Lecture Series: Energy Systems for Space Application SS 2020*. 2020.
- [8] S. Klinkner; P. Winterhalder, and M.Nitz et al. *Lecture Series - Rover System Technology SS2021*. 2021.
- [9] SAFT Batteries. *Datasheet - SAFT MP 176065 xlr*. 2018. [online] [\url{https://www.saftbatteries.com/products-solutions/products/mp-small-v1}](https://www.saftbatteries.com/products-solutions/products/mp-small-v1).
- [10] Bradford Space. *Datasheet - Nova PCDU*. Ed. by BRADFORD ENGINEERING BV. 2019. [online] [\url{https://satsearch.co/products/bradford-nova-pcdu}](https://satsearch.co/products/bradford-nova-pcdu).

Appendix

A Electrical Power System

SAFT 176065 xlr [9]	
Configuration:	
Battery Configuration	4s3p
Cells in Series s N [-]	4
Cells in Parallel p M [-]	3
Cell Parameters:	
Typical Cell Capacity [Ah]	6.8
Nominal Cell Voltage [V]	3.65
Nominal Cell Capacity [Wh]	24.8
Typical Cell Mass [kg]	0.15
Energy Density [Wh/kg]	165.33
Actual Battery Configuration Parameters:	
Battery Voltage V_{Batt} [V]	14.6
Battery Nominal Capacity E_{Batt} [Wh]	297.6
Battery Mass [kg]	1.8
Battery Mass m_{Batt} (incl. 10% Margin) [kg]	1.98
Configuration according to ECSS reliability restrictions and margins included:	
Battery Configuration	4s2p
Cells in Series s N [-]	4
Cells in Parallel p M [-]	2
Battery Voltage V_{Batt} [V]	14.6
Battery Nominal Capacity E_{Batt} [Wh]	198.4
30% Margin on Energy Content	0.3
Battery Nominal Capacity E_{Batt} incl. Margin [Wh]	138.88
Useable Energy Density [Wh/kg]	70.14

Table A.1: INSPIRE battery parameters.

S/C Net Power Demand [W]	Margin (%)				2.76		24.86		16.90		3.86			30.30		3.25			157.60			17.73			14.09
Power Distribution loss	2.00%				0.06		0.50		0.34		0.08			0.61		0.07			3.15			0.35			0.28
Load Discharge (PCDU)	7.00%				0.19		1.74		1.18		0.27			2.12		0.23			11.03			1.24			0.99
PCDU Margin (Conversion etc.)	5.00%				0.14		1.24		0.85		0.19			1.52											
Harness losses	3.50%				0.10		0.87		0.59		0.14			1.08		0.11			5.52			0.62			0.49
Additional losses	5.00%				0.14		1.24		0.85		0.19			1.52		0.16			7.88			0.89			0.70
S/C Brutto Power Demand [W]					3.38		30.45		20.70		4.73			37.12		3.82			185.18			20.83			16.55
System Margin	20.00%				0.68		6.09		4.14		0.95			7.42		0.76			37.04			4.17			3.31
Required power from Battery (20% System Margin) [W]					4.06		36.54		24.84		5.67			44.54		4.58			222.22			24.99			19.86
Total Rover Power Demand excluding battery charge (Battery Charge Loss 5% + Lion Efficiency 5%) [W]	10.00%				4.46		40.20		27.33		6.24			49.00		5.04			244.44			27.49			21.85
Incoming Power RTG	-				12.08		12.08		12.08		12.08			12.08		12.08			12.08			12.08			12.08
Total Rover Power Demand including battery charge [W]	-				-7.62		28.12		15.25		-5.84			36.92		-7.04			232.36			15.41			9.77

Figure A.1: POWER BUDGET DUMMY

B Thermal Controls System

B.1 Heat energy equilibrium

The following equations describe each node of the thermal network. The input values were taken from EPS or from Subsection B.2, Subsection B.3, Subsection B.4.

RTG:

$$\begin{aligned} \dot{Q}_{RTG} + CON_1 \cdot (T_{Bay} - T_{RTG}) + CON_2 \cdot (T_{Chassis} - T_{RTG}) + CON_5 \cdot (T_{Drill} - T_{RTG}) - \\ - \epsilon_{RTG} \cdot \sigma_b \cdot S_{RTG} \cdot T_{RTG}^4 = 0 \end{aligned}$$

Electric Bay:

$$\dot{Q}_{Bay} + CON_1 \cdot (T_{RTG} - T_{Bay}) + CON_3 \cdot (T_{Chas} - T_{Bay}) - \epsilon_{Bay} \cdot \sigma_b \cdot S_{Bay} \cdot T_{Bay}^4 = 0$$

with:

$$\dot{Q}_{B,intern} = \dot{Q}_{C\&DH} + \dot{Q}_{Tranceiver} + \dot{Q}_{Receiver} + \dot{Q}_{PCDU}$$

Drill & Analyser:

$$\dot{Q}_{Drill} + CON_4 \cdot (T_{Chas} - T_{Drill}) + CON_5 \cdot (T_{RTG} - T_{Drill}) = 0$$

Camera:

$$\begin{aligned} \dot{Q}_{Cam} + \dot{Q}_{RHU} + CON_6 \cdot (T_{Chas} - T_{Cam}) + (CON_{14} + n_{S1} \cdot CON_{S1}) \cdot (T_{Rad} - T_{Cam}) - \\ - \epsilon_{Cam} \cdot \sigma_b \cdot S_{Cam} \cdot T_{Cam}^4 = 0 \end{aligned}$$

Radiator:

$$(CON_{14} + n_{S1} \cdot CON_{S1}) \cdot (T_{Cam} - T_{Rad}) - \epsilon_{Rad} \cdot \sigma_b \cdot S_{Rad} \cdot T_{Rad}^4 = 0$$

Chassis:

$$\begin{aligned} \dot{Q}_{Radar} + \dot{Q}_{Hazcam} + CON_2 \cdot (T_{RTG} - T_{Chas}) + CON_3 \cdot (T_{Bay} - T_{Chas}) + \\ + CON_4 \cdot (T_{Drill} - T_{Chas}) + CON_6 \cdot (T_{Cam} - T_{Chas}) + CON_7 \cdot (T_{Node1} - T_{Chas}) + \\ + \alpha_{Chas} \cdot [q_{Sun} \cdot (1 + \rho_E) \cdot (S_{Chas1} \cdot \varphi_1 + S_{Chas2} \cdot \varphi_2) + \epsilon_E \cdot \sigma_b \cdot S_{Chas3} \cdot T_{Surface}^4] - \\ - \epsilon_{Chas} \cdot \sigma_b \cdot S_{Chas} \cdot T_{Chas}^4 = 0 \end{aligned}$$

Steer Engine:

$$4 \cdot [\dot{Q}_{E,S} + (CON_8 + n_{S2} \cdot CON_{S2}) \cdot (T_{Node1} - T_{E,S}) + CON_9 \cdot (T_{RTG} - T_{E,S}) - \epsilon_{E,S} \cdot \sigma_b \cdot S_{E,S} \cdot T_{E,S}^4] = 0$$

Distribution Node 1:

$$4 \cdot [CON_7 \cdot (T_{Chas} - T_{Node1}) + CON_8 \cdot (T_{E,S} - T_{Node1}) + CON_{10} \cdot (T_{Node2} - T_{Node1})] = 0$$

Drive Engine:

$$4 \cdot [\dot{Q}_{E,D} + (CON_{11} + n_{S3} \cdot CON_{S3}) \cdot (T_{Node2} - T_{E,D}) + CON_{12} \cdot (T_{RTG} - T_{E,D}) - \epsilon_{E,D} \cdot \sigma_b \cdot S_{E,D} \cdot T_{E,D}^4] = 0$$

Distribution Node 2:

$$4 \cdot [CON_{10} \cdot (T_{Node1} - T_{Node2}) + CON_{11} \cdot (T_{E,D} - T_{Node2}) + CON_{13} \cdot (T_{Ground} - T_{Node2})] = 0$$

B.2 Heat conductance

B.3 Heat switch

The characteristic of the switch conductance depends on the mean temperature T_M , shown by measurements in cite . As this temperature wont be calculated in the analysis, the corresponding component temperature T_C shall be used. In order to describe the characteristic, it was divided in three sections, Figure B.2. The temperature where the disk decouples is $T_{toggle} = 108K$ and not applicable for the current application. By reducing the heigt, the toggle temperature can be increased and the characteristic can be shifted to higher temperatures ("to the right"). It was assumed, that the gradients of section 2 and 3 as well as the temperature range of section 2 keep constant. The axis intersection is a function the toggle temperature ($a_2 = f(\Delta T_{toggle})$, $\Delta T_{Toggle} = T_{new} - T_{old|toggle}$).

Section	Temperature range	Heat conductance $C_t = \frac{1}{R_t}$
1	$T_{toggle} > T_C$	$C_{t,1} = 16.4 \cdot 10^{-3} \frac{W}{m^2 K} = const.$
2	$T_{toggle} \leq T_C < T_1$	$C_{t,2}(T_C) = a_{1,1} \cdot T_C + a_{1,2}$ $a_{1,1} = +1.272 \cdot 10^{-3} \frac{W}{m^2 K^2}$ $a_{1,2} = -1.272 \cdot 10^{-3} \frac{W}{m^2 K^2} \cdot \Delta T_{Toggle} - 0.117 \frac{W}{m^2 K}$
3	$T_C > T_1$	$C_{t,3}(T_C) = a_{2,1} \cdot T_C + a_{2,2}$ $a_{2,1} = +333 \cdot 10^{-6} \frac{W}{m^2 K^2}$ $a_{2,2} = -333 \cdot 10^{-6} \frac{W}{m^2 K^2} \cdot \Delta T_{Toggle} - 28.3 \cdot 10^{-3} \frac{W}{m^2 K}$

Table B.2: Sections and range of the switch characteristic.

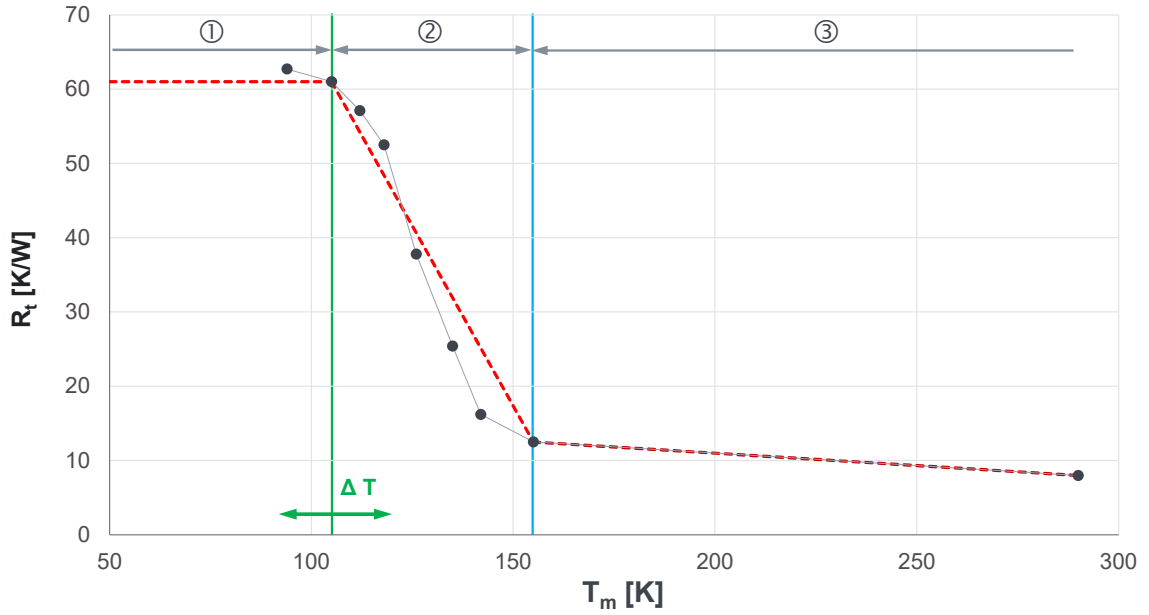


Figure B.2: Switch characteristic divided in sections.

B.4 Rover absorptivity

The amount of solar radiation onto the rover depends on the sun altitude, see [autoref\(fig:tcsabsop\)](#).

View Factor 1, Inclination: $\varphi_1 = \cos(\lambda) \cdot \cos(\delta)$
View Factor 2, Declination: $\varphi_2 = \cos(90^\circ - \lambda) \cdot \cos(\delta)$

B.5 Values

Component	Temperature limits in [$^\circ C$]	
	min.	max.
Command & Data Handling		
Transmitter	-10	50
Receiver	-30	70
PCDU	-40	60
Battery	-35	60
Camera	-40	70
Objektive	-40	71
Steering Engine	-30	100
Steering Gear	-30	85
Drive Engine	-40	100
Drive Gear	-40	100

Table B.3: Temperatur limits of the rover components.

The Europas ground temperature varies at the equator between $T_{e,min} = 80K$ and $T_{e,max} = 130K$, depending on the sun inclination. The temperature at the pole is $T_{Pole} = 50K$, cite(europa). It was assumed, that the ground temperature depends on the sun altitude. A trigonometrical interpolation was defined as follows.

$$T_{Ground}(\lambda, \delta) = T_{Pole} + \cos(\delta) \cdot [(T_{e,min} + \cos(\lambda) \cdot (T_{e,max} - T_{e,min})) - T_{Pole}]$$

For λ and δ see Subsection B.4.

Surface finishing	Emisivity [-]		Absorptivity [-]		Source
	min.	max.	min.	max.	
Aluminium, polished	0.045				
Sand blasted alloy					
White paint					

Table B.4: Minimum and maximum of surface emisivity and absorptivity values.

Material	Nominal	Used	Source
Aerogel	0.002 - 0.05	0.05	
Aluminium	236	236	
Copper ²⁾	400	360	
Steel ²⁾	21 - 50	21	

¹⁾ a reduction of 10% was considered

²⁾ depends on the alloying component, a conservative value was chosen

Table B.5: Heat conductivity in $\frac{W}{mK}$

Part	Description	Value m^2
------	-------------	-------------

Table B.6: Radiation surface of components.

C Radiation

In this chapter, detailed calculations are performed on which Section 4.7 is based on. All calculations and figures in Section C are performed with SPENVIS unless otherwise stated. In order to simulate the radiation on Europa an orbit around Jupiter is simulated with the orbit parameters of Europa with a total mission duration of 30 days. The chosen parameters were an perijove altitude of 664,862 km, an apojove altitude of 676,938 km, and an inclination of 0.47.

C.1 Jupiters Radiation Environment

In order to compare the radiation environment around Jupiter and the radiation environment around Earth the following trapped radiation models were used: for Jupiter the D&G83+Salammbo proton model and D&G83+GIRE+SalammboE electron model was used; for Earth the AP-8 proton model and the AE-8 electron model was used.

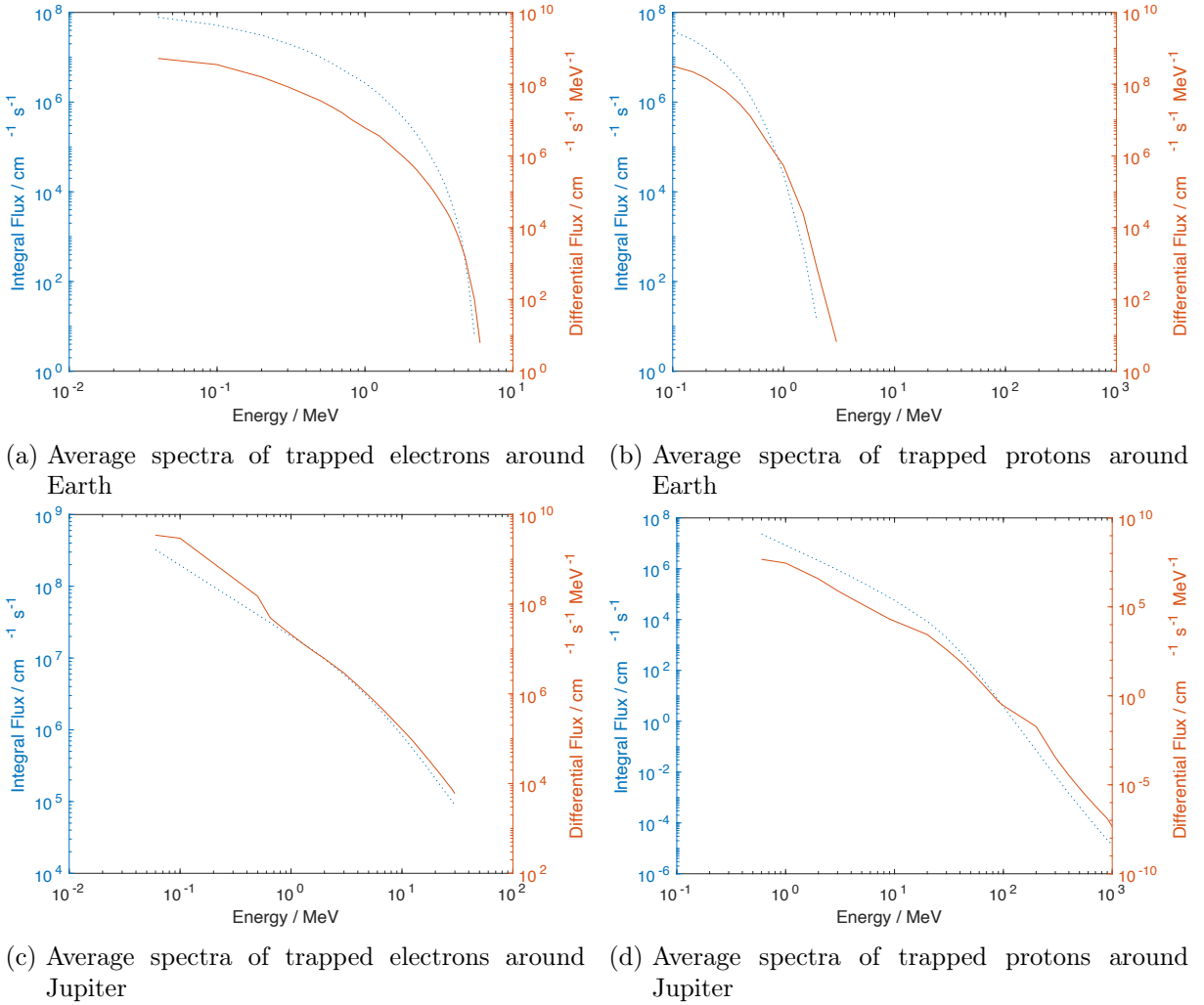


Figure C.3: Average trapped proton and electron fluxes on an orbit around earth at 25,000 km, through the outer Van Allen radiation belt, and on Europa's orbit around Jupiter.

C.2 Radiation Exposures

In order to simulate the TID for different radiation protections the Geant4 tool Multi-Layered Shielding Simulation (MULASSIS) is used. As target material silicon is selected with a thickness of $1\ \mu\text{m}$. As shape a planar slap is selected because of the ice ground on one side of the rover.

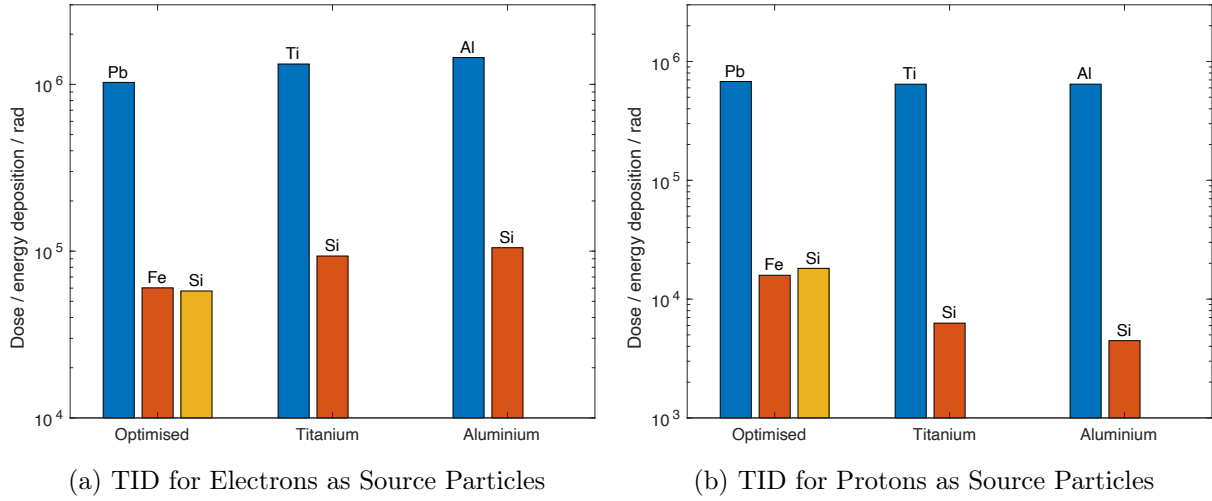


Figure C.4: TID of aluminium, titanium, and the optimised radiation structure shown in Table 4.5 with a weight target of all three structures of $0.5\ \text{g}/\text{cm}^2$ over 30 days of exposure on Europa.

Table C.7: Used components and the respective radiation tolerance and location

Components	Rated TID	Exposed TID	Location
Electric Motors	-	$< 205\ \text{krad}$	locomotion housing
Harness	-	$< 98\ \text{krad}$	chassis
Stereo Vision Cams	40	$< 31\ \text{krad}$	camera housing
OBC	1000	$< 17\ \text{krad}$	E-Bay
PCDU	20	$< 17\ \text{krad}$	E-Bay

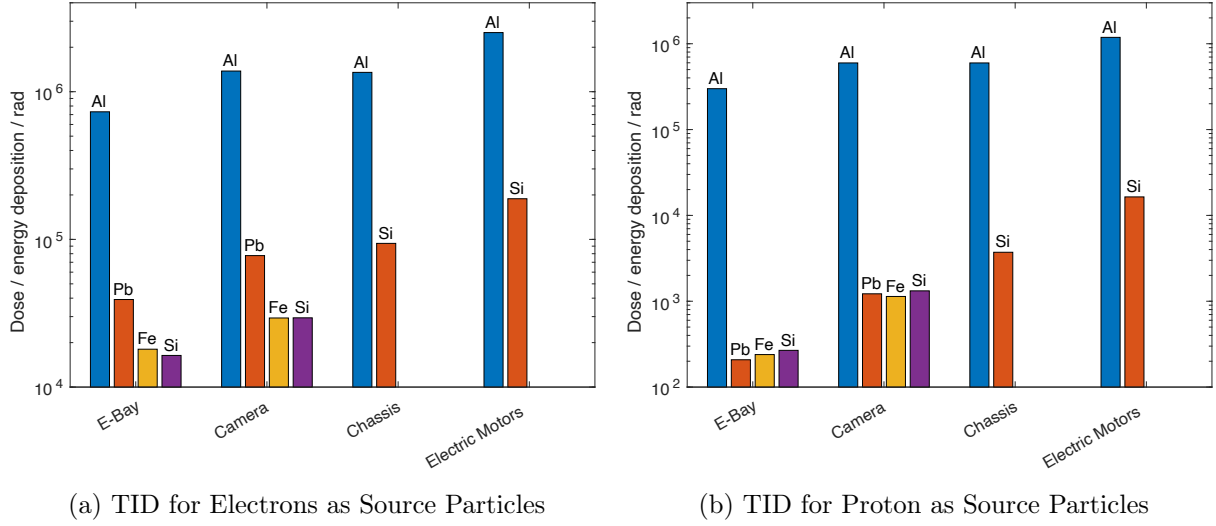


Figure C.5: TID for different compartments as seen in Figure 4.6. The E-Bay is shielded by 4 mm aluminium, 0.415 mm lead, and 0.033 mm iron; the camera compartment by 2 mm aluminium, 0.415 mm lead, and 0.033 mm iron; the chassis by 2 mm aluminium; the electric motors by 1 mm aluminium.

C.3 Improvements

All simulations of the improvements introduced in Subsection 4.7.3 are performed in the same way as in Subsection C.2.

In Figure C.6, the TID over 30 days within the E-Bay is shown. If all components with an radiation resistance under 43.27 krad are shielded individually, the additional shielding structure around the E-Bay can be removed and the aluminium structure would be sufficient.

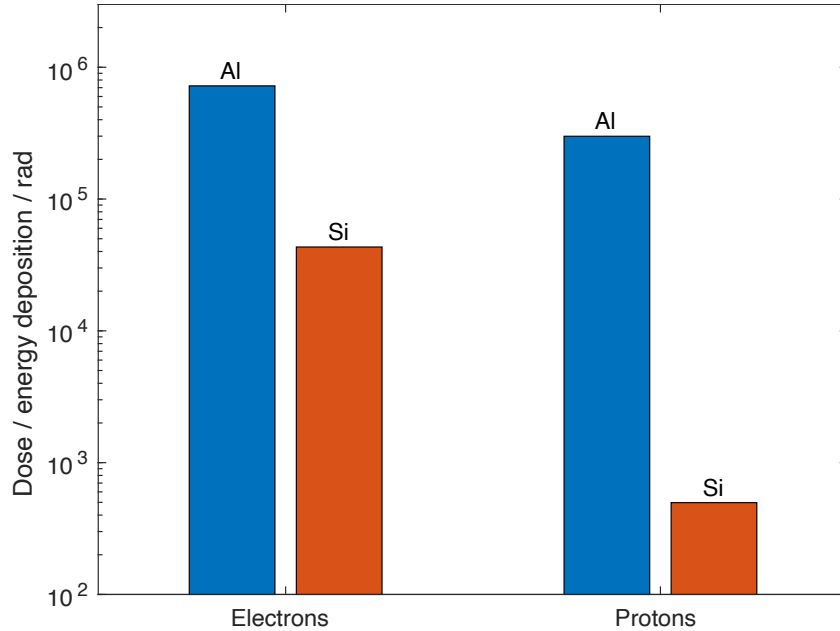


Figure C.6: TID with 4 mm Al shielding over a mission duration of 30 days

The resulting mass savings can be calculated with Equation 5.1 with m^* as the specific weight of the radiation protection and N as the amount of components within the E-Bay with a radiation

resistance under 43.27 krad as of Table C.7.

$$\Delta m = SA_{\text{E-Bay}} \cdot m_{\text{Shielding}}^* - \sum_{n=0}^N SA_{\text{Component, n}} \cdot m_{\text{Shielding}}^* \quad (5.1)$$

With inserted values this results in a mass saving of $\Delta m = 736.2$ g.

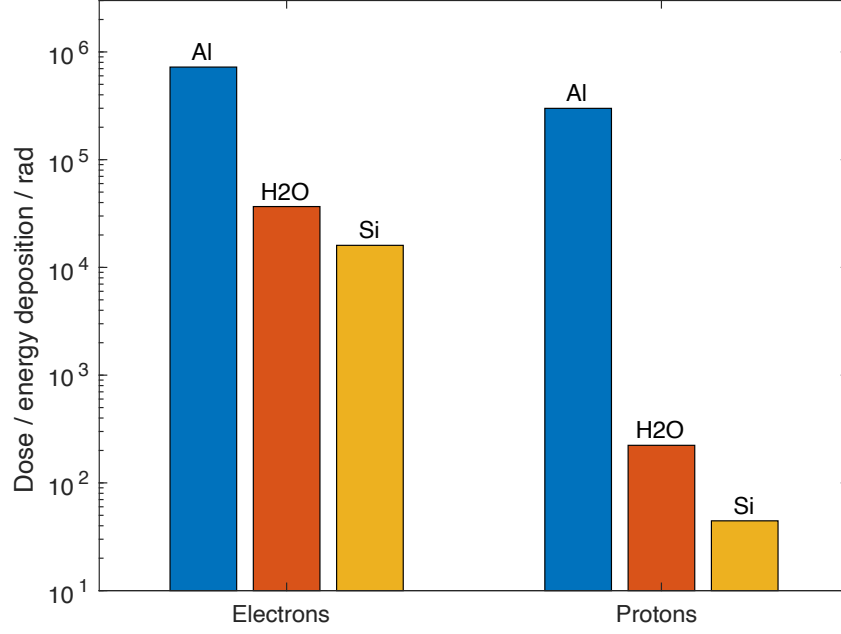


Figure C.7: TID with 4 mm Al shielding and 1 cm of Water over a mission duration of 30 days

